Streamflow Hysteresis Analysis through a Deep Dive Budget

of the St Venant Momentum Terms

Emma House[a], Ehab Meselhe[a], Marian Muste[b], and Ibrahim Demir[a]

[a] Tulane University: 6823 St Charles Ave, New Orleans, LA 70118, U.S.A., ehouse@tulane.edu, emeselhe@tulane.edu, idemir@tulane.edu.

[b] University of Iowa: IIHR-Hydroscience & Engineering, C. Maxwell Stanley Hydraulics Laboratory, Iowa City, IA 52245, U.S.A., kyeongdong-kim@uiowa.edu, marian-muste@uiowa.edu.

Corresponding Author: Emma House ehouse@tulane.edu

Abstract

Hysteretic conditions entail non-unique time-independent relationships in flow variables and are prevalent in the unsteady flow regime of most rivers worldwide. Estimation errors associated with the inability of current monitoring techniques to resolve hysteresis effects could have profound implications when the recorded data is used for water resources management and flood forecasting. A deep analysis of streamflow hysteresis is performed by tracking the St Venant momentum equation terms for storm events propagating at several locations along the Illinois River, USA, using a combined 1D/2D hydraulic model. We correlate flow characteristics with magnitude and timing patterns in these terms to determine their relevance to the presence and absence of hysteretic conditions. The dynamic equation analysis confirms that the hysteretic behavior is related to certain defining characteristics in momentum terms. The local acceleration term only temporally advances the flood wave and is not an indication of hysteretic behavior. Non-hysteretic streamflow has large and balanced gravity and friction forces, equating it to kinematic wave conditions. Meanwhile, hysteretic streamflow has a clear disparity between gravity and friction forces, balanced by active diffusive and convective acceleration forces. In such hysteretic conditions, the diffusive, convective acceleration, and friction slope terms exhibit non-unique relationships and a peak-phasing phenomenon much like the hysteresis signature of the hydraulic variables used to estimate streamflow. For non-hysteretic conditions, the relationships are purely unique and linear, with synchronized variable peaks. The revealed flow characteristics provide information on the important drivers of streamflow hysteresis and create opportunities for improving streamflow monitoring and forecasting.

Plain Language Summary

Streamflow hysteresis occurs during flood events in mildly sloped rivers and results in flows during the build-up of the event being larger than those during the flood recession for a given water level. This presents a complexity not captured by the simplistic assumptions of current streamflow monitoring protocols and prompts further research into the drivers of streamflow hysteresis. Using numerical model simulations with various hysteretic signals, we examine various terms of the governing equations for 1D flow. Through this, we identify differences in the underlying flow regime of streamflow for a range of streamflow conditions. It is seen that non-hysteretic streamflow behaves as kinematic flow while hysteretic streamflow has active diffusive and dynamic terms. We also see a peak-phasing in the momentum terms in hysteretic streamflow. The uncovered flow characteristics in hysteretic streamflow may be utilized for improved streamflow estimation and forecasting.

1 Introduction

In riverine monitoring and flood prediction, a critical challenge persists in the need for accurate streamflow data and timely forecasts (Demir et al., 2022). Streamflow data is used for flood forecasting (Krajewski et al., 2021; Sit et al., 2021), inundation mapping (Li & Demir, 2022), water quality constituents (Jones et al., 2018), sediment studies (Xu et al., 2019), reservoir management, and more. The USGS introduced continuous streamflow monitoring to the United States in the early 1800s (Follansbee, 1944). In the past 200 years, there have been incremental developments in the measurement protocols used for continuously collecting streamflow data. Most methods are based on relationships constructed with steady flow assumption that are not valid during unsteady flows. These semi-empirical relationships (a.k.a. rating curves) relate continuously measured hydraulic variables such as stage, index velocity, or free-surface slope with streamflow (Rantz, 1982; Levesque and Oberg, 2012; Holmes, 2016; Muste et al., 2019).

The most used streamflow monitoring method is the century-old stage-discharge rating, which is based on underlying physics that has hardly received scientific justification. This has resulted in widely recognized problems in developing and applying ratings in unsteady flows, hence requiring a variety of empirical adjustments that are applied after the data is collected (Schmidt & Garcia, 2013). The only source of accurate data on unsteady flow is obtained by directly measuring the discharge with instruments such as Acoustic Doppler Current Profilers (ADCP). Given that streamflow data acquired with ADCP, or any other instruments, are too costly and time-intensive to feasibly use for continuous in-situ measurements, the rating-based methods continue to be used for monitoring steady and unsteady flows. Currently, there are no systematic studies to detect the presence of hysteresis during flood wave propagation nor rigorous investigations to identify the physical reasons for documented shortcomings in ratings. This study aims to investigate the natural dynamics of unsteady streamflow to support developments of monitoring methods that open the door to more accurate estimations and forecasts.

1.1 Streamflow Hysteresis

Hysteresis in river streamflow occurs during unsteady flow conditions when the water surface slope changes due to rapidly rising or falling water levels in a channel. Most pronounced in mild sloped streams exposed to large flood waves, hysteresis introduces a non-unique relationship among flow variables during the phases of flood wave propagation. This peak-phase effect and “loop rating curve” (Figure 1), reflects a larger streamflow (for the same stage) during the rising limb than the falling limb of the hydrograph (Henderson, 1966; Dottori et al., 2009, Muste et al., 2020). Additionally, for the same discharge, the river stage is higher during the falling limb than the rising limb. This noted complexity presents a variation from the steady-state assumptions used in the current protocols for estimating streamflow.

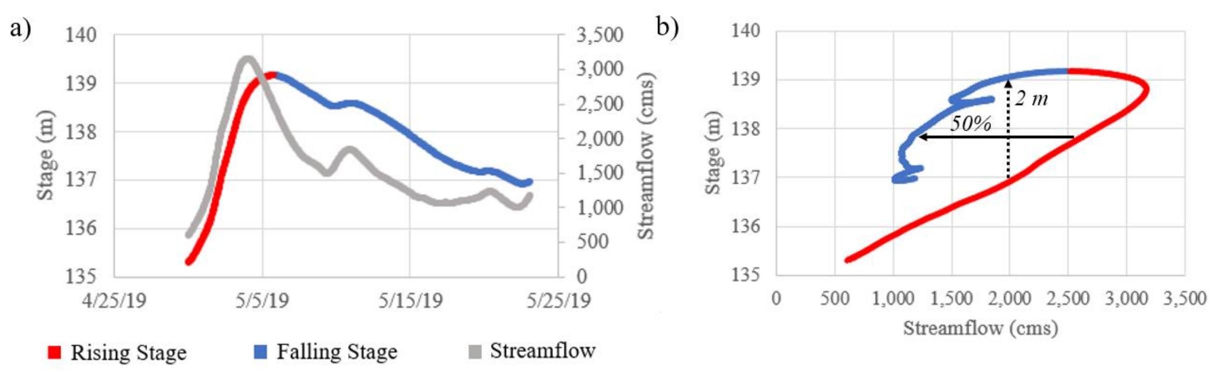

Figure 1. Model-simulated hysteretic streamflow data for the Illinois River at Henry, IL for a summer 2015 storm event, a) hydrographs of stage and streamflow, and b) stage-discharge rating curve. The rising and falling limbs of the stage hydrograph are distinguished using color in both plots to show the approximately 50% decrease in flow for a given stage (plain arrow), and 2-meter increase in stage for a given flow (dotted arrow), between the rising and recession limbs.

Overlooking hysteretic channel flow dynamics causes estimation errors that are inadequately considered epistemic uncertainties and being most often larger than the <5% typically accepted in the current monitoring protocols (Schmidt, 2002). Hysteretic conditions are present in the unsteady streamflow regime of 67% of rivers gaged with the stage-discharge method by the USGS (Holmes, 2016). Hysteresis effects due to flood waves can lead to as much as 65% error in measurements with conventional methods (Muste et al., 2022a). Furthermore, unsteady flows can last for up to 50% of the annual streamflow cycle in low-gradient rivers (Muste et al., 2024). Since hysteresis is so prevalent in natural channels, errors of this magnitude have profound implications on flood forecasting and water resources management.

1.2 Conventional Rating Curve Methods

While the stage-discharge rating curve HQRC method is accurate for steady flows, the actual flows can depart considerably from the estimates with HQRC in unsteady flows (Kennedy, 1984; Fenton, 2001). Monitoring agencies are aware of the limitations of the HQRC performance when monitoring unsteady flows and/or in the presence of backwater (Rantz et al., 1982). Consequently, new methods are tested and implemented for monitoring these more complex flows (Holmes, 2016). Currently, there are several conventional and emerging monitoring methods including the widely used stage-discharge (HQRC) approach and the index-velocity (IVRC) method which, as of 2011, is used to estimate streamflow for 470 USGS stations (Levesque and Oberg, 2012; Holmes, 2016). Due to its inclusion of index velocity, a dynamic flow characteristic, IVRC is better suited than HQRC for estimating unsteady streamflow (Cheng et al., 2019). The Continuous Slope Area (CSA) method utilizing continuous water surface slope measurements to estimate streamflow has been tested by Smith et al. (2010) and subsequently validated with field conditions and numerical simulations by Lee et al. (2017) and Muste et al. (2019).

The HQRC monitoring method can be corrected for hysteresis through post-processing algorithms that involve additional in-situ measurements (Rantz et al., 1982; Schmidt & Garcia, 2003). However, due to the correction costs, they are currently only applied to rivers in major flood-prone areas where the gaging stations support streamflow forecasting (Muste et al., 2022b). Due to the limitations of current methods, novel approaches for accurately estimating streamflow will continue to be developed. Improvements in instrumentation technology within the last few decades can help to narrow the gap between our current knowledge of cyclical flow dynamics and the protocols for continuous monitoring and forecasting streamflow. This study makes an effort along this line by analyzing fine details of the unsteady flow dynamics that inform on the strategy to be adopted for accurate streamflow monitoring with considerations of the local conditions at the measurement sites.

1.3 Essentials of Hysteresis Behavior

To characterize streamflow properly, it is critical to reveal the hysteretic behavior of flow variables. Hysteresis is currently identified by two well-documented phenomena: 1) the non-unique relationships between flow variables for the rising and falling stages of flood wave propagation (Figure 1), and 2) the sequential peak-phasing of the flow variables: water surface slope, velocity, discharge, and stage (Figure 2, Graf and Qu, 2004; Muste et al., 2022a). The later hysteretic feature is observed in simulations with hydraulic models using unsteady flow engines but is rarely captured with field measurements due to the complexity of such an undertaking.

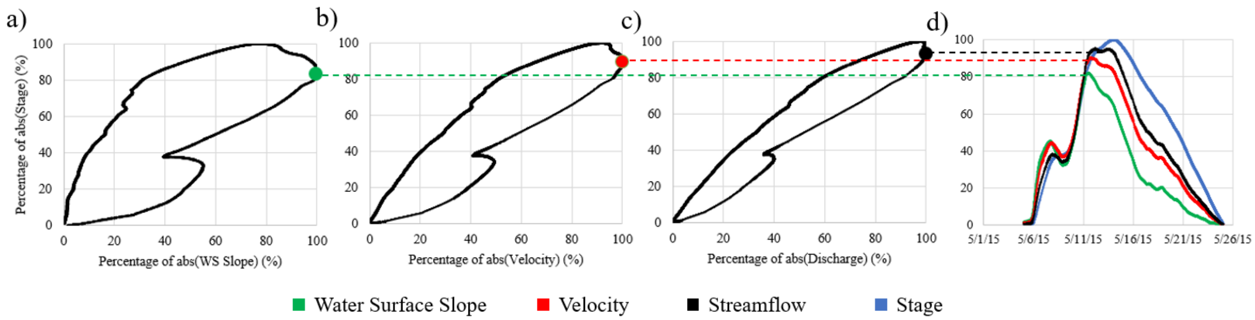

Figure 2. Model-simulated hysteretic streamflow data for the Illinois River at Henry, IL a) stage vs. water surface slope, b) stage vs. average cross-sectional velocity, c) stage vs. discharge, and d) sequential peak-phasing for an event in 2015 (after Muste et al., 2022).

Hydrographs of these variables in hysteretic streamflow are both unique and sequential in time: characteristics that can be utilized in both streamflow estimation and forecasting (Muste et al., 2022b). For example, the dynamic terms, water surface slope, and velocity peaking early in hysteretic reaches can be great predictors for machine learning streamflow forecasting algorithms. There may be further defining and useful features of hysteresis that may be uncovered using numerical models. Diving deeper into the flow physics, there may be a link between the relative magnitude of the full-dynamic equation momentum terms and the formation of hysteretic behavior.

1.4 Momentum Terms

The continuity (Eq. 1) and momentum (Eq. 2) equations are relevant in streamflow estimation, as together they represent the governing De Saint Venant equations for 1D flow which conserve mass and momentum or energy, depending on the formulation used (de St Venant, 1871; Knight, 2005; Muste et al., 2020; Meselhe et al, 1997). Friction and gravity forces make up the kinematic term of the equation while the acceleration and pressure gradient, representing the dynamic and diffusive terms, respectively, account for unsteadiness in the streamflow stage and velocity in the streamwise direction. Several studies have focused on the separation of these forces within the exploration of wave types and flow routing to identify the applicability of various forms of the St Venant equations (Ferrick et al., 1985; Meselhe et al., 2021).

$$\frac{\partial Q}{\partial x} + \frac{\partial A}{\partial t} = 0 \tag{1}$$

$$\frac{\partial Q}{\partial t} + \frac{\partial}{\partial x}\left(\frac{Q^2}{A}\right) + gA\frac{\partial y}{\partial x} + gA\left(S_0 - S_f\right) = 0 \tag{2}$$

where Q is discharge, A is cross-sectional area, x is distance along the channel, t is time, y is depth, g is the gravity constant, S_0 is bed slope, and S_f is friction slope. In (2), local acceleration $\frac{\partial Q}{\partial t}$ and convective acceleration $\frac{\partial}{\partial x}\left(\frac{Q^2}{A}\right)$ make up the dynamic momentum term, $gA\frac{\partial y}{\partial x}$ is the pressure gradient or diffusive term, and $gA\left(S_0 - S_f\right)$ is the balance of gravity and friction forces which makes up the kinematic term. The contributions of these terms to the overall budget in the momentum equation applied to various sites and event intensities define the type of fluvial wave passing throuhg the site at various instances, i.e., kinematic, diffusive or dynamic.

There is further work to be done on the parameterization of flow variable relationships contributing to hysteresis, so this study uses process-based numerical models to reproduce the hydraulic dynamics in unsteady flows to better understand the phenomenon. By providing more detail and robustness than is attainable with direct measurements, essential evidence-based support is provided to inform flood monitoring and management decisions.

To achieve reliable results from a modeling-based study, it is important to ensure that models are performing according to physics and observed data. We hypothesize that streamflow hysteresis can be represented with numerical simulations if the proper form of the governing equations, timestep, channel geometry, and boundary conditions allow for this.

The validated physics-based model output will provide valuable insights toward answering the question of whether there is a discernable difference between the significance of individual momentum terms between hysteretic and non-hysteretic streamflow. We hypothesize that there is a direct link between the relative magnitudes of the momentum terms and the presence or absence of hysteretic behavior. Just as the non-kinematic St Venant terms are negligible in steady-uniform flow, some terms may have defining characteristics in hysteretic streamflow.

2 Materials and Methods

In a process-based modeling approach, several numerical models are combined to produce the output that constitutes this study. A large hydraulic model and accompanying set of reduced complexity models simulate streamflow of varying hysteretic intensity.

2.1 Illinois River Hydraulic Model

The primary study area for this analysis is the Illinois River, which has a variable slope and many interactions with lakes, pools, channels, and backwater conditions. The complexity of the riverine system makes hysteresis dynamics present and variable, which is why the vast extent of the Upper Mississippi River (UMR) system is a suitable study area.

The primary model used as a basis for this study is set up as a 1D/2D Hydrologic Engineering Center River Analysis System (HEC-RAS) model developed by the US Army Corps of Engineers (USACE), as the Phase III portion of the UMR Flood Risk Management hydraulic model system (USACE, 2022). Its intended purpose is to inform risk management decisions for the UMR Watershed Plan. The model extends from Lockport Lock and dam at Lockport, IL to the Illinois River’s confluence with the Mississippi River at Grafton, MS (Figure 3). The simulations perform unsteady computations by using the ID unsteady finite difference numerical solution and the 2D unsteady diffusion wave equation.

Study locations for this analysis are highlighted in Figure 3. Located on straight reaches, these locations are represented by 1D channel geometry in the model so that the St Venant equations are applicable to capture the full flow dynamics. These locations also have varying channel and flow characteristics. For example, the flow at Marseilles, IL downstream of the Marseilles lock and dam (Mars_DS) can generally be characterized by a steady stage-discharge rating curve, while the station at Henry, IL is observed to have a large loop rating curve with rising streamflow larger than falling streamflow for a given stage. These two stations will represent the non-hysteretic and hysteretic streamflow for the analysis, respectively.

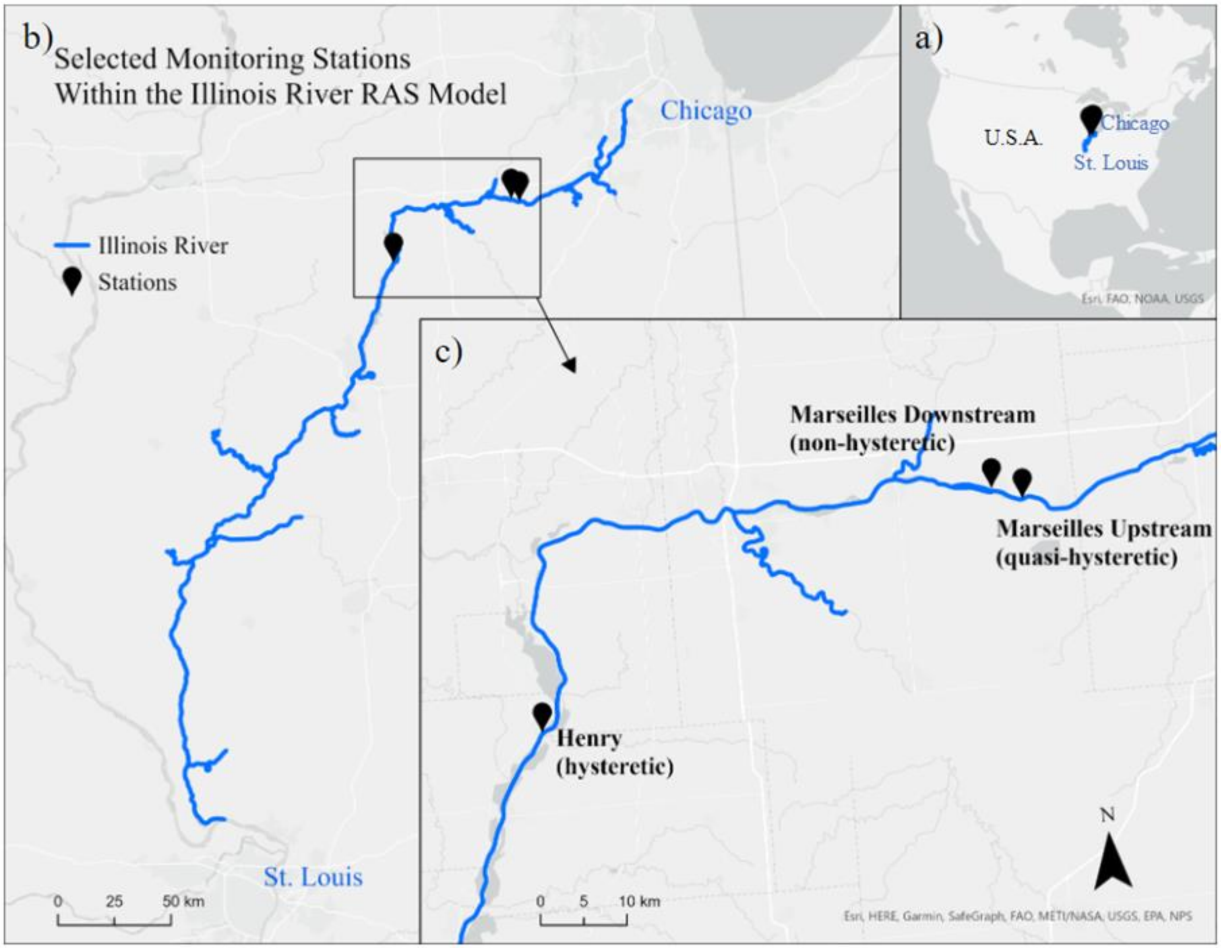

Figure 3. An overview map of a) the United States, b) the Illinois River RAS model extent with monitoring station case study locations, and c) case study locations and their preliminary hysteresis classification highlighted.

The Illinois River RAS model has input data from a wide range of sources. Light Detection and Ranging (LiDAR) data with horizontal resolution of 1-m resampled to 2-m was used to create the topographic-bathymetric layer (USACE, 2022). Manning's roughness coefficients vary spatially for 1D and 2D model elements, determined using the National Land Cover Database (NLCD). Bridges, ineffective flow areas, levees, and dams are accounted for using lateral structures and 2D flow areas. Hydrologic inflow data at the mainstem boundaries and major tributaries are sources from the USGS and USACE monitoring sites on the river. Finally, a North Central River Forecast Center conceptual model estimates inflows for approximately 20% of the area which has no measured observations. This setup results in a well-performing model that is useful for both practical applications and scientific studies.

2.2 Flood Events

The two flood events of focus for this study were moderate to major events for the Illinois River. The larger event in summer 2019 reached its peak streamflow at approximately 3,000 cms at Henry, IL, and the water level exceeded bankfull elevation (BE) at all locations studied here. The smaller event in summer 2015 had a peak streamflow of approximately 900 cms and did not exceed bankfull elevation at any of the locations studied. The validation plots in

Figures 4 and 5 demonstrate that the Illinois River RAS model matches the observed (IVRC for estimating streamflow) time series for the 2019 event at two of the study locations (Muste and Kim, 2021).

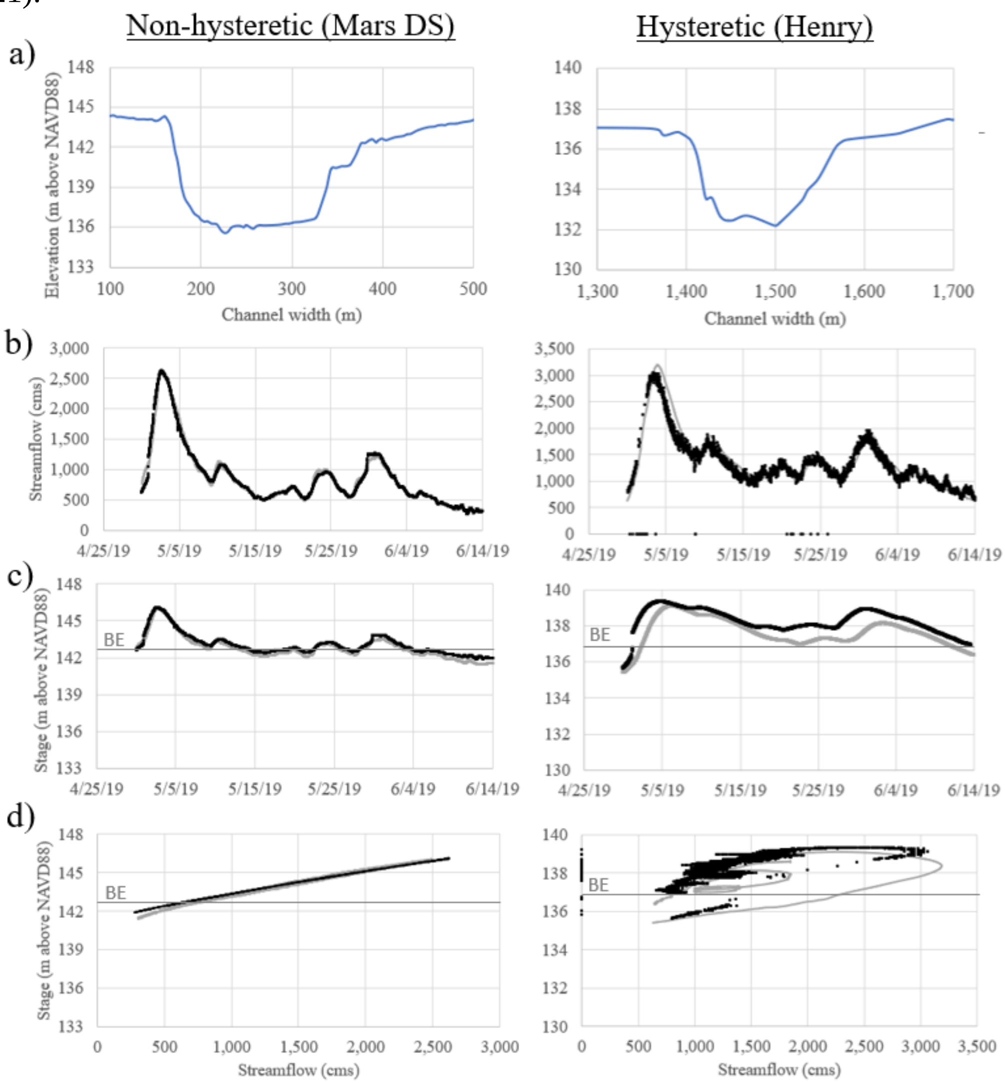

Figure 4. Model validation plots showing field (USGS) observations (black) and model simulations (gray) for locations exhibiting non-hysteretic and hysteretic behavior on the Illinois River: a) cross section plots, b) streamflow time series, c) stage time series, and d) the stage-discharge rating curves for the 2019 event. Bankfull elevation (BE) as defined in the Illinois River RAS model is indicated on the stage axes.

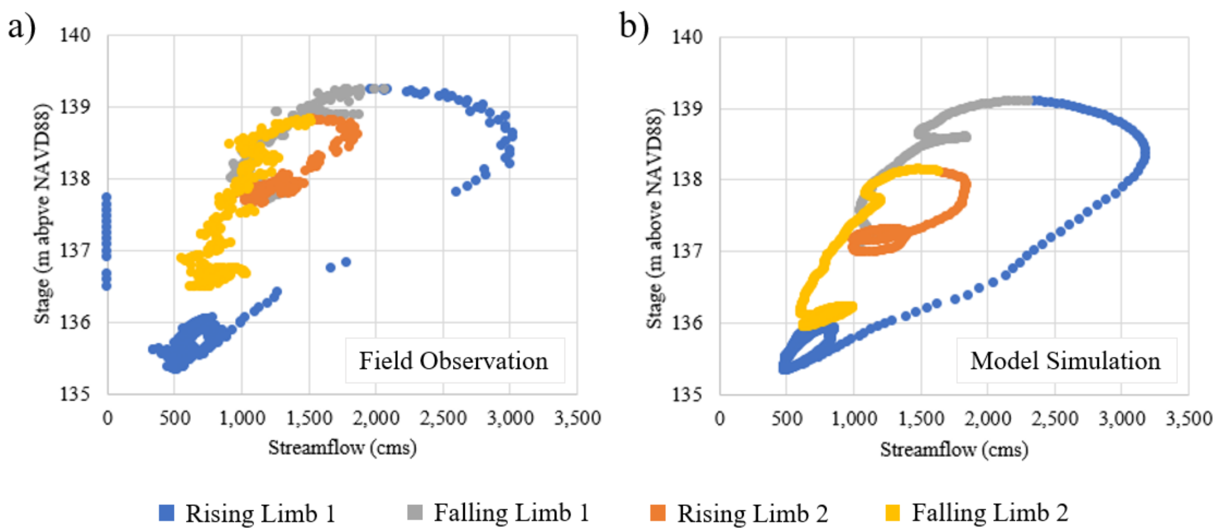

Figure 5. Model validation plots showing stage-discharge rating curves from a) field (USGS) observations, and b) model simulations for a location exhibiting hysteretic behavior on the Illinois River (Henry, IL) for the multi-pulse 2019 event with the rising and falling limbs for the two peaks differentiated in color.

2.3 Reduced Complexity Models

Using numerical models, it is possible to explore changes in flow regime during the hysteretic cycle throughout the length of a modeled reach. Variation in streamflow hysteresis in the Illinois River is a great case study to guide hysteresis parameterization. However, the USACE Illinois River RAS model is computationally heavy with many features that complicate this detailed of an examination.

To gain more control over the analysis, reduced complexity models are created for each area of interest along the Illinois River. Two benefits of these models are 1) the interpretation of the result is clearer, and 2) using these representative models increases the capacity for more detailed simulations with short run times. Using a simple rectangular cross-section and a long (10km), straight channel, characteristics such as bed slope, channel width, roughness, and smoothed boundary condition time series are transferred from the Illinois River RAS model to reduced complexity models that represent a single reach. Three reaches are selected for comparison here based on their wide range of hysteretic signals. A reach at Marseilles, IL downstream of the lock and dam generally exhibits non-hysteretic streamflow and is represented by a steep bed slope of 0.002, width of 250 m, and Manning’s n roughness of 0.04. Marseilles, IL upstream of the dam has a quasi-hysteretic streamflow, mild bed slope of 0.00022, width of 350 m, and n = 0.025. Finally, Henry, IL exhibits a strong hysteresis signal, with a mild bed slope of 0.00027, width of 450 m, and n = 0.025. It is important to note that these models use the full St Venant equations.

To study flow dynamics throughout the streamflow hysteresis cycle, the individual terms of the momentum equation (Eq. 2) are calculated using outputs from the reduced complexity models at a high temporal frequency. With the output time series (flow, velocity, cross-sectional area, water surface and friction slopes, etc.) of an unsteady simulation, the individual terms (local acceleration, convective acceleration, pressure gradient, friction forces, and gravity forces) can be examined. Drawing correlations between channel characteristics, boundary conditions, and the relative magnitudes of the momentum terms forms the results of this study.

3 Results

The hypotheses are addressed with experimental simulations of the Illinois River RAS model and reduced complexity numerical models.

3.1 Hysteresis Representation in Models

We check that streamflow hysteresis is accurately represented in these reduced complexity numerical simulations by 1) looking for the known hysteresis characteristics, looped relationships and peak variable phasing, and 2) confirming that there is no violation of the laws of physics.

Streamflow hysteresis can be accurately represented in simulations of the full IL River RAS model, as seen in the distinctly accurate representation of the characteristic loop and variable phasing in the hysteretic condition (Figures 4-5). Additionally, the reduced complexity models represent physics without many of the complexities burdening the original model (Figure 6). With this confirmation, we can reliably study the streamflow hysteresis loops intensifying and collapsing as fluvial flood waves travel down the Illinois River.

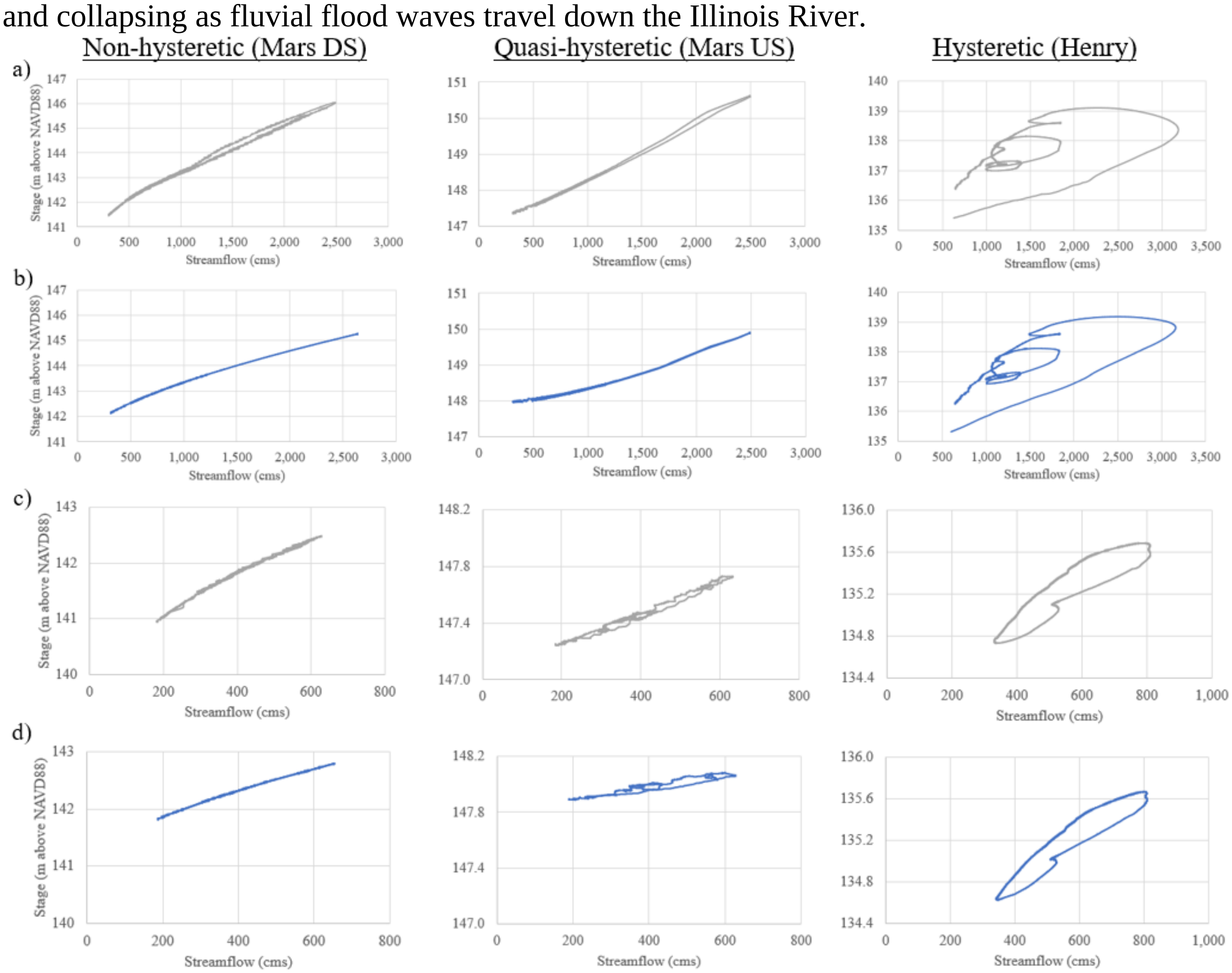

Figure 6. Preservation of physics plots for the IL River model (gray) and reduced complexity model (blue) for the a-b) 2019 and c-d) 2015 events.

The spatial-temporal resolution of the simulations must reliably capture the relevant dynamics to perform an assessment of the momentum terms during the hysteretic cycle. We confirm that the conservation of momentum (2) holds true by dividing the absolute value of each momentum term by the sum of the absolute values of all the terms. For each of the reduced complexity models, we ensure that the resulting residual error is small (<1%) and that the output does not change with a further resolved time or space step. The resulting common setup for the reduced complexity models is a simulation with dx = 300 meters and dt = 1 minute.

3.2 Kinematic, Diffusive, and Dynamic Momentum Terms

To begin examining momentum terms, we compare output from the reduced complexity models for the three locations. Figures 7-8 are time series of momentum terms which have correlations to hysteresis strength.

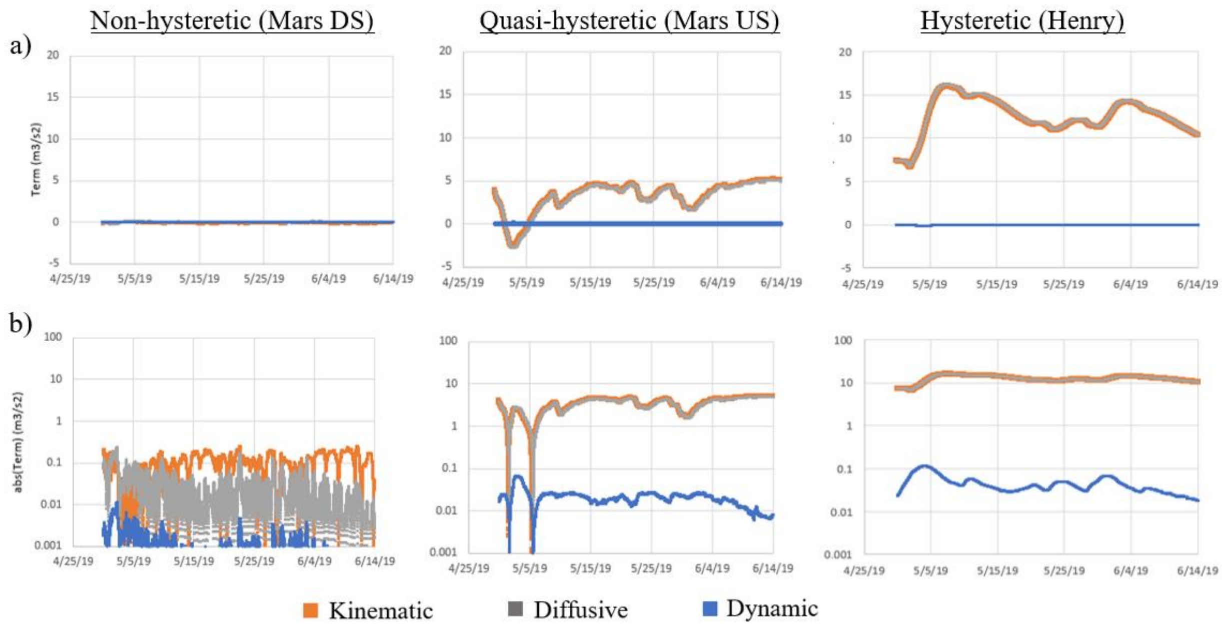

Figure 7. Momentum term breakdown showing terms in a) their native values, and b) their absolute values on a semi-log scale for three locations on the Illinois River for the 2019 event.

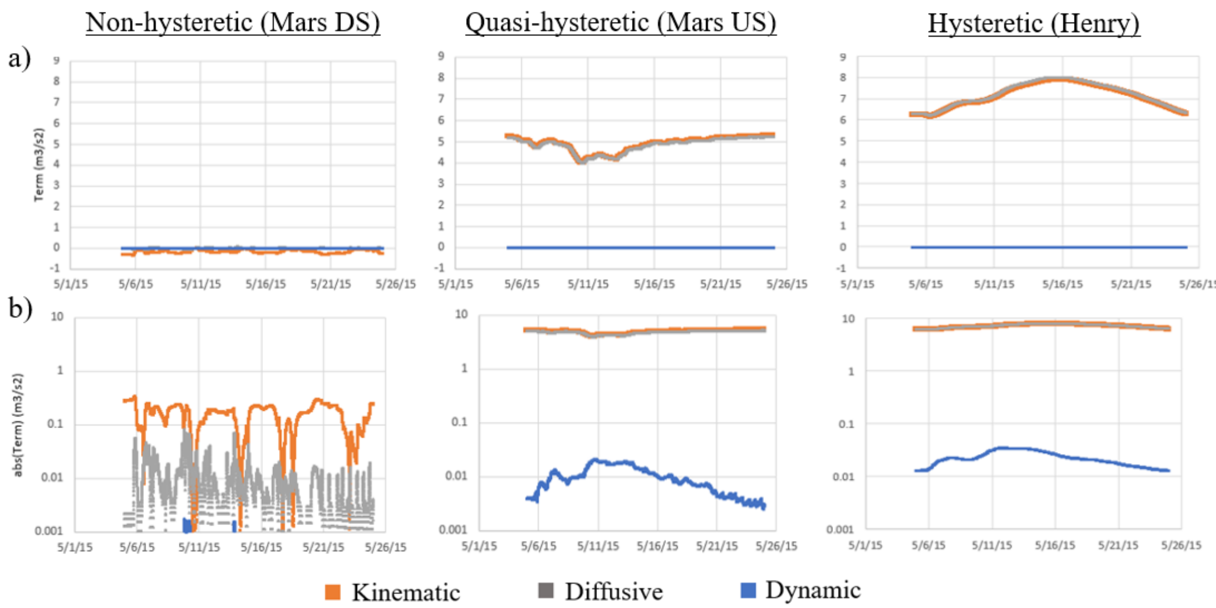

Figure 8. Momentum term breakdown showing terms in a) their native values, and b) their absolute values on a semi-log scale for three locations on the Illinois River for the 2015 event.

When examining the kinematic, diffusive, and dynamic terms as the first level of breaking down the momentum terms, several observations can be made. The terms are all very small in the non-hysteretic condition, with a kinematic term near 0.1 m^3/s^2 and negligible diffusive and dynamic terms. In the hysteretic condition, kinematic and diffusive (bulk) terms are comparable and 2-3 orders of magnitude larger, and the dynamic term is active, around 0.01 m^3/s^2. There is also a sequential peak-phasing observed in the dynamic-bulk terms in the hysteretic simulation. Although they are significantly out of balance in magnitude, the dynamic term peaks a few days before the bulk terms in the hysteretic simulation. This phenomenon is most pronounced in the bottom right plot of Figures 7-8.

3.3 Momentum Term Ingredients

To further explore the kinematic, diffusive, and dynamic momentum terms, their ingredients (namely, local acceleration, convective acceleration, pressure gradient, gravity, and friction forces) are examined for these three stations and two events. Several key findings are demonstrated in Figures 9-12 in the time series of momentum term ingredients.

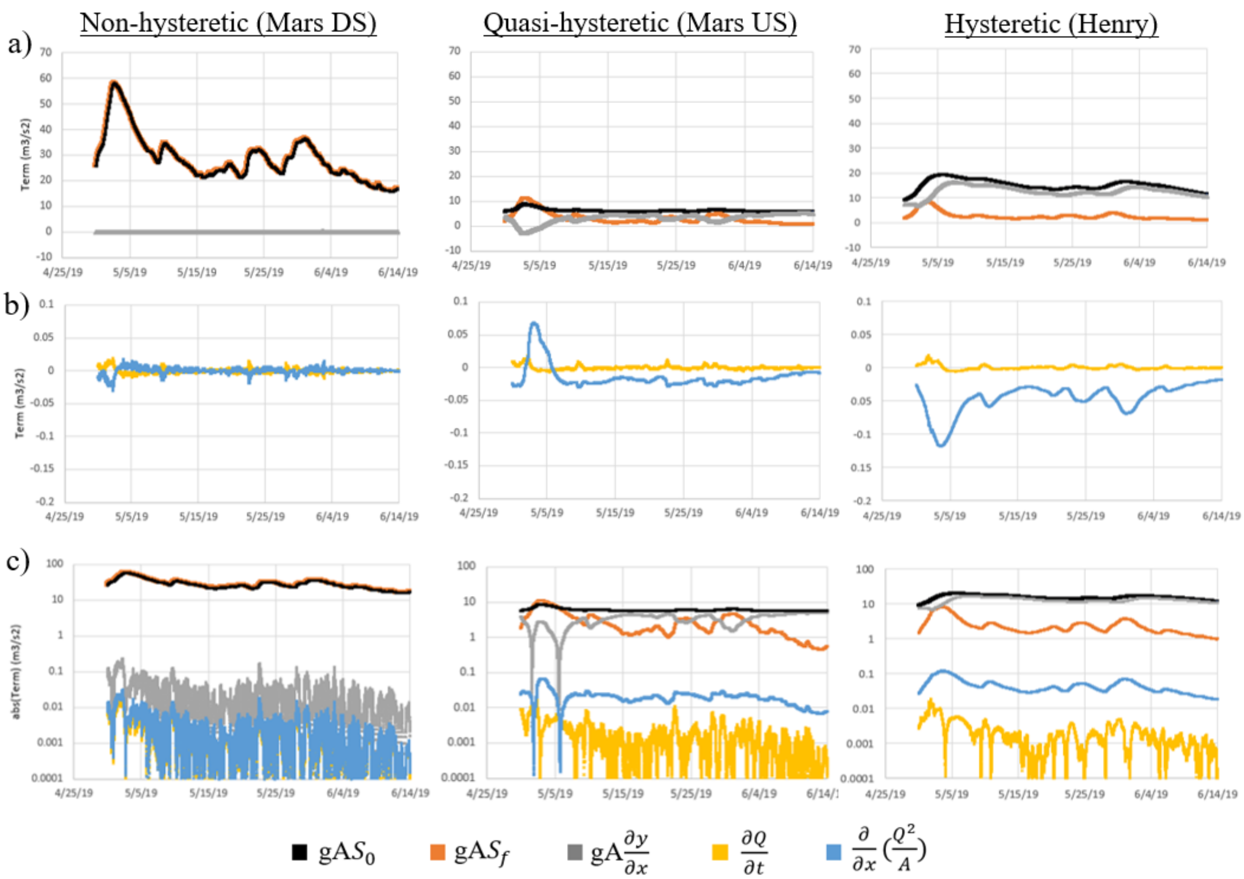

Figure 9. Momentum term ingredients of the a) kinematic and diffusive terms, b) dynamic terms in their native values, and c) their absolute values on a semi-log scale for three locations on the Illinois River for the 2019 event.

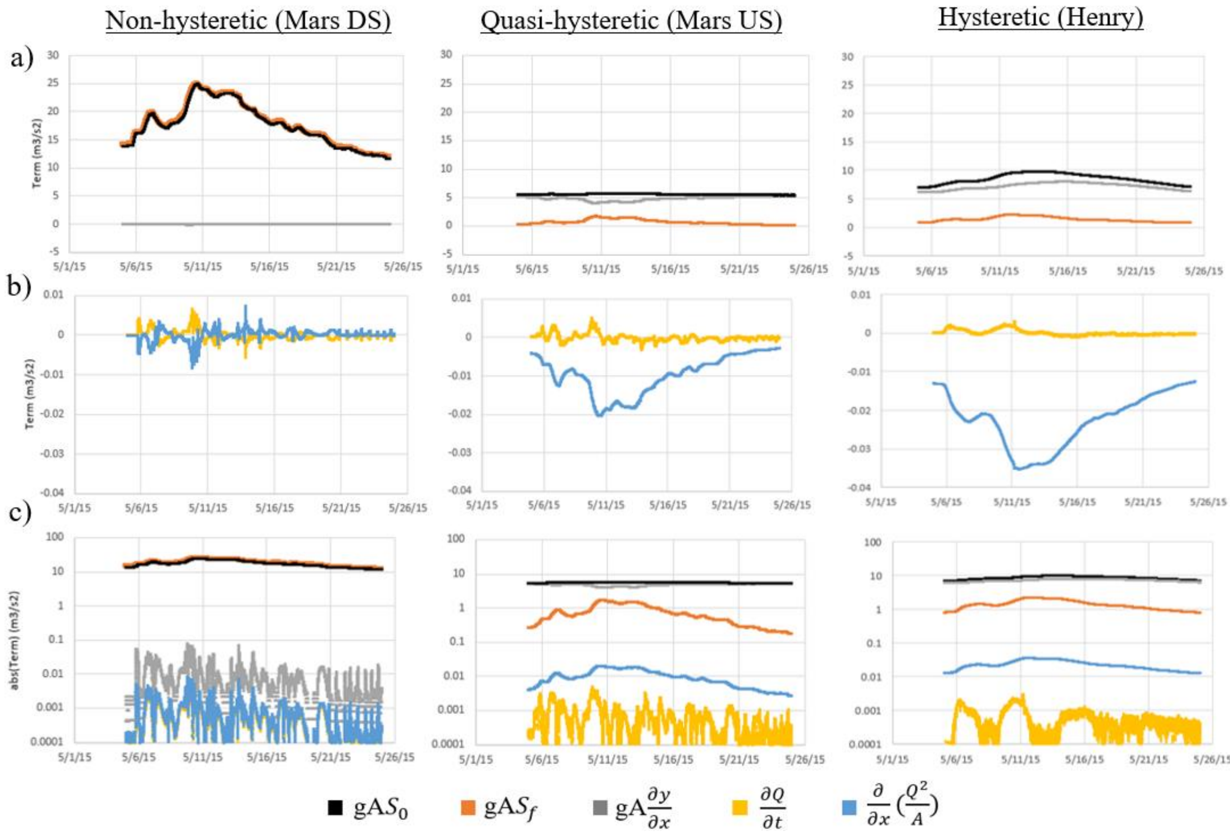

Figure 10. Momentum term ingredients of the a) kinematic and diffusive terms, b) dynamic terms in their native values, and c) their absolute values on a semi-log scale for three locations on the Illinois River for the 2015 event.

The kinematic term exhibits an interesting behavior. In the hysteretic condition, the kinematic term, in totality, is much larger than in the non-hysteretic condition (Figures 7-8). However, when diving deeper into the active forces, the individual kinematic ingredients themselves are essentially large and balanced in the non-hysteretic reach, leading to the misleadingly small total kinematic term (Figures 9-10, left). Meanwhile, the kinematic wave ingredients are smaller and out of balance in hysteretic conditions, with friction forces one order of magnitude smaller than gravity forces (Figures 9-10, middle and right). When hysteresis is present, the diffusive term is comparable in magnitude and the convective acceleration term is significant enough to even out the imbalance of the overall dynamic equation. Resultingly, the diffusive and dynamic terms are significant in hysteretic streamflow while they are negligible in non-hysteretic streamflow.

In hysteretic streamflow, it has been observed that there is a sequential peak phasing observed in the streamflow variables (Figure 2) and now the dynamic-bulk terms (Figures 7-8). Through this analysis we see that there is also a clear phasing in the ingredients of the momentum equation terms (Figures 11-12).

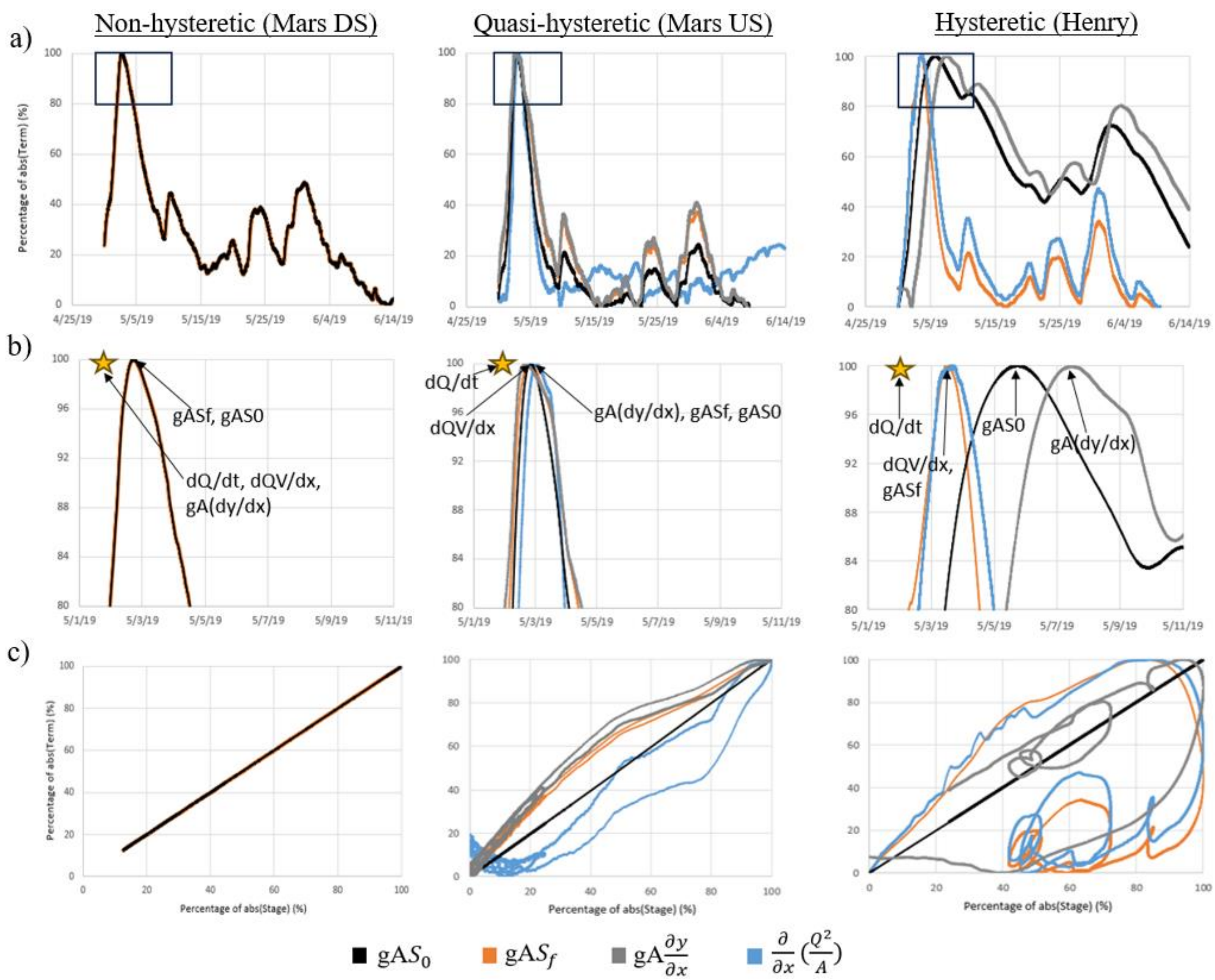

Figure 11. Peak phasing for a) the whole event, b) the 10-day period around the hydrograph peaks, and c) loop relationships of the momentum term ingredients for three locations on the Illinois River for the 2019 event.

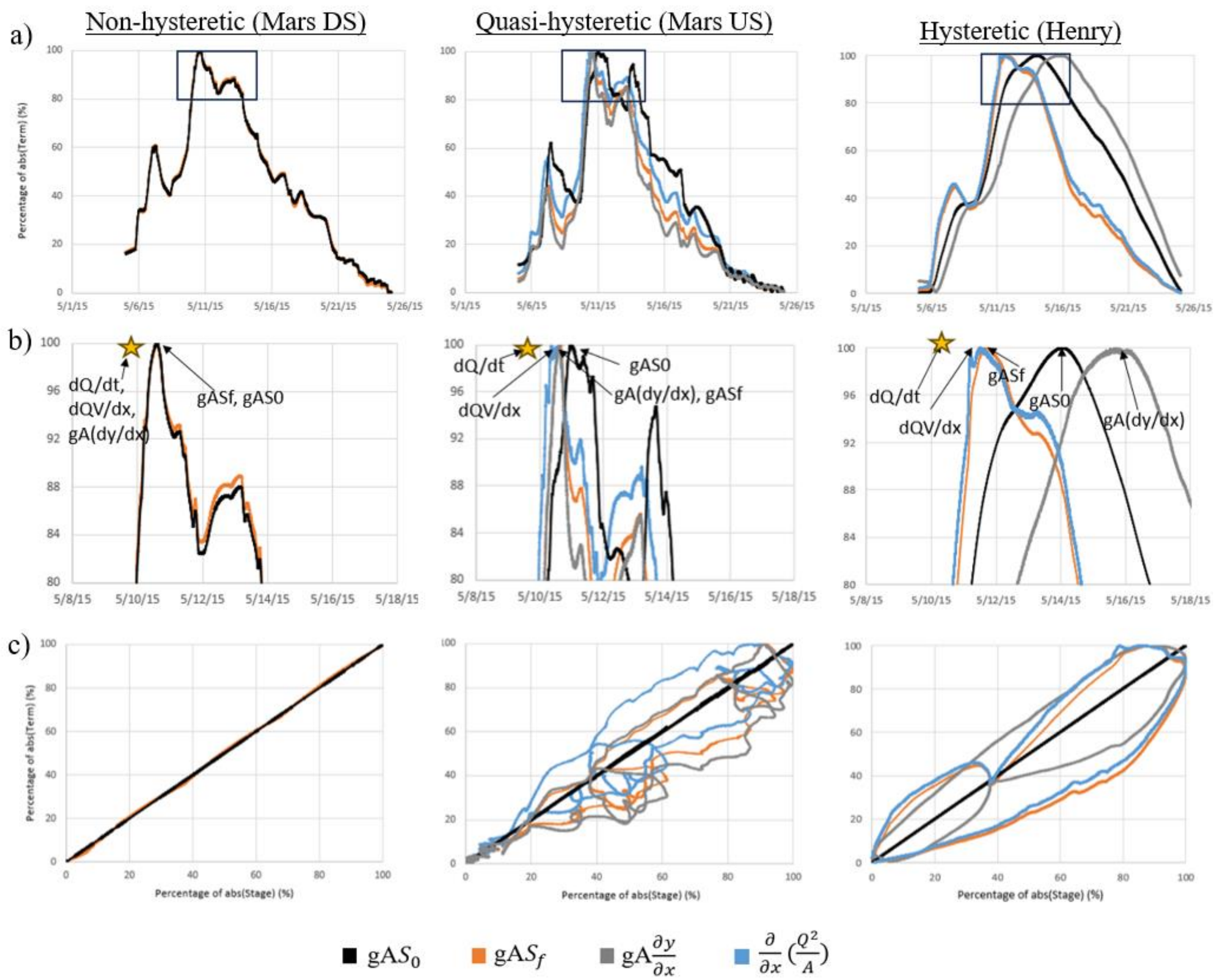

Figure 12. Peak phasing for a) the whole event, b) the 10-day period around the hydrograph peaks, and c) loop relationships of the momentum term ingredients for three locations on the Illinois River for the 2015 event.

In non-hysteretic streamflow, the active momentum term ingredients peak concurrently. With strengthening hysteretic intensity, the time between peaks increases. In all cases, the dynamic term ingredients peak first, followed by friction then the gravity forces. The pressure gradient is seen to peak later with increasing hysteretic intensity, with a lead time of about 5 days from the first momentum ingredient peaks in the hysteretic condition for both events shown.

3.4 Flow Variables

After making several observations on the underlying physics of streamflow hysteresis through a budget of the momentum terms, it is useful to link these findings to flow characteristics that are measurable in the field. For the two flood events, water surface slope, average cross-sectional velocity, streamflow, and stage are seen to peak sequentially in time in the quasi-hysteretic and hysteretic streamflow conditions (Figures 13-14).

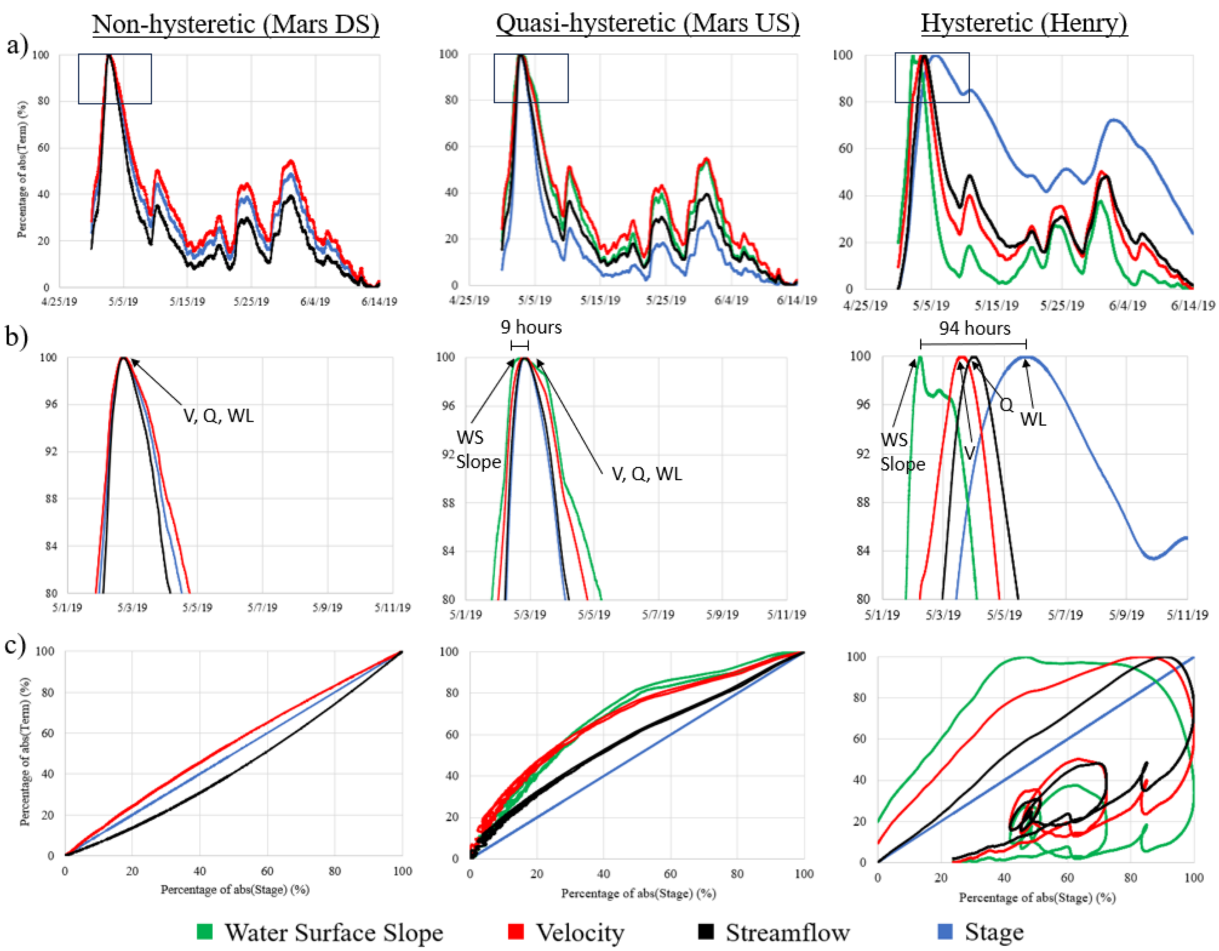

Figure 13. Phasing for a) the whole event, b) the 10-day period around the hydrograph peaks with the time between the first and last variable peak, and c) loop relationships of the flow variables for three locations on the Illinois River for the 2019 event.

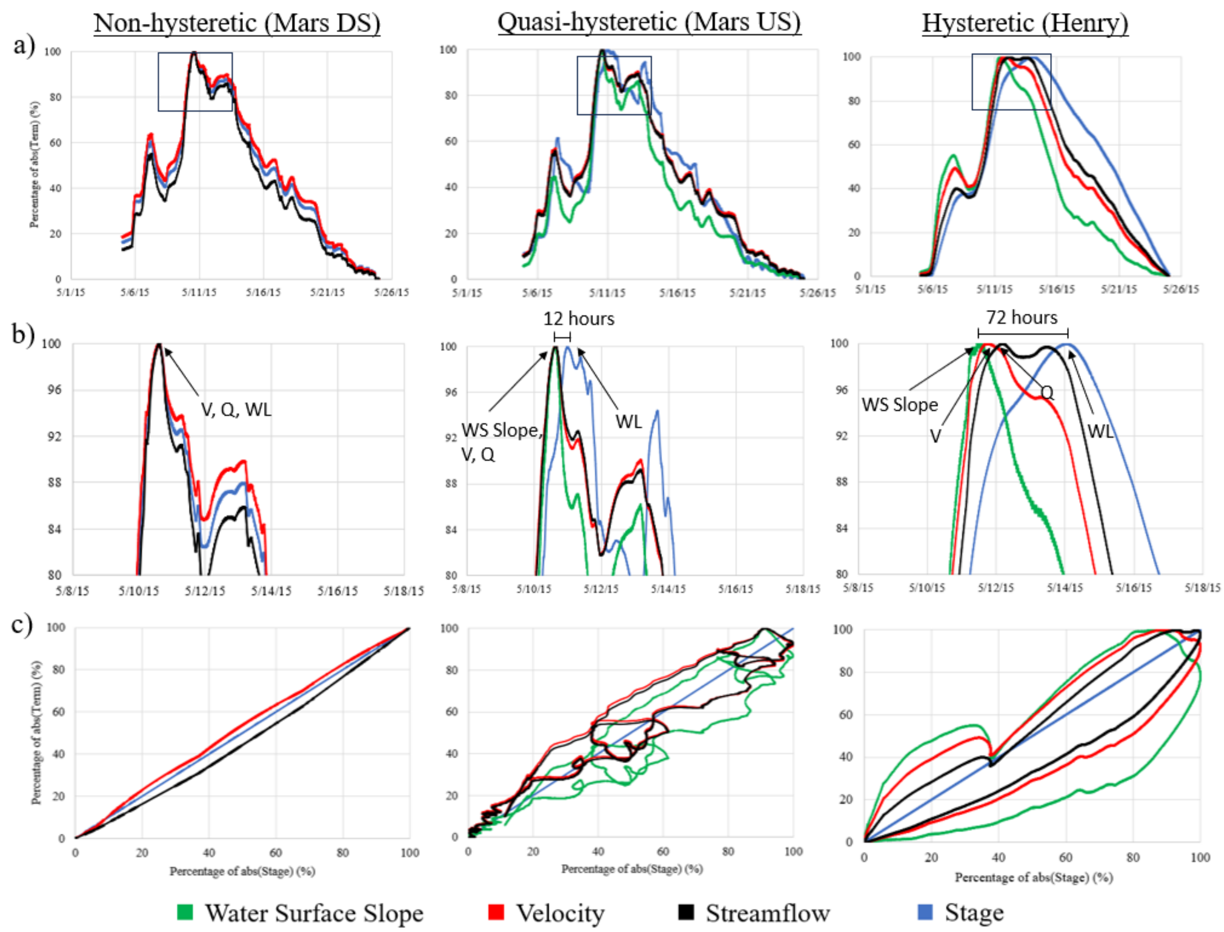

Figure 14. Phasing for a) the whole event, b) the 10-day period around the hydrograph peaks with the time between the first and last variable peak, and c) loop relationships of the flow variables for three locations on the Illinois River for the 2015 event.

Confirming the literature, not much peak-phasing seen is in the flow variables for non-hysteretic streamflow, while increasingly hysteretic streamflow introduces a sequential peak-phasing phenomenon. In the hysteretic condition, there is up to a 4-day lead time between the peaks of water surface slope and stage for the flow conditions examined here. These inferences are informative on the variables that are important in the monitoring methods to account for the hysteretic behavior.

4 Discussion

This study takes a deep dive into the momentum terms for streamflow with varying signals of hysteresis through representation in numerical models, examining the momentum terms, their ingredients, and flow variables.

4.1 Hysteresis Representation in Models

The experience here proves that we can use process-based numerical models to study complex dynamics of streamflow as long as the computational time step and output interval are sufficiently small to allow for accurate estimation of the temporal and spatial gradients (Figures 4-5). Further, we ensured that transitioning from the full Illinois River model to the reduced complexity model did not alter the physics. As such, we verified that forcing a reduced complexity model with hydraulic boundary conditions preserved the hysteretic and non-hysteretic signals (Figure 6).

Aspects of the hysteretic streamflow are adequately conserved such as the effects of overbank flow and multi-peak storm events. The reduced complexity models increase computational efficiency, thereby opening the door to deep analyses of streamflow variables. It should be emphasized that we focused on locations of the Illinois River system where the flow was predominantly one-dimensional so that the St Venant equations fully represent the flow dynamics.

4.2 Momentum Terms Deep Dive

In looking deeper into the St Venant terms for streamflow of varying hysteretic signals, several strong patterns are observed. The relative magnitude and timing of the kinematic, diffusive, and dynamic terms and their ingredients give rise to different hysteretic conditions in the streamflow commensurate with the site bed slope and event intensity. This finding has implications for understanding the drivers of streamflow hysteresis and the application of appropriate monitoring and modeling methods.

The kinematic term ingredients, S_o and S_f, representing the balance between gravity and friction, are strongest in non-hysteretic streamflow where they are in balance and in-sync temporally (Figures 9-10). Thus, it can be inferred that non-hysteretic streamflow behaves in a kinematic nature. Meanwhile, hysteretic streamflow has smaller, unbalanced kinetic terms and active diffusive and dynamic terms (Figures 7-10). It seems that the imbalance in kinematic terms allows for the more complex terms to become significant in the momentum equation. As hysteresis strength increases, we have found that the disparity in kinematic terms increases in magnitude and timing (Figures 9-10). Accordingly, the diffusive and convective acceleration term seems to be directly related to the strength of the hysteresis loop, as those values increase to make up for the kinematic imbalance. These findings reveal the patterns within hysteresis and the underlying drivers: the imbalance of gravity and friction and the increasing dominance of convective acceleration forces.

The temporal phasing of the momentum term ingredients is also important for hysteresis development. We can identify differences between the phasing for varying strengths of the hysteresis signal (Figures 11-12). In the non-hysteretic condition, the kinematic term ingredients that are active are synchronized, while those variables that are out of phase are very small in magnitude. Thus, non-hysteretic streamflow is considered to involve no phasing of the momentum terms. Meanwhile, hysteretic streamflow presents a clear peak-phasing phenomenon in momentum terms. As evident considering the study locations in order of strengthening hysteresis intensity, the temporal spread between variables increases; the longer lag time between peaks translates into larger loop thicknesses in variable relationships. In the hysteretic condition, the local acceleration term invariably peaks first, followed by convective acceleration, friction, gravity, and finally pressure forces. The early peaking of those more influential dynamic forces and the later peaking of the diffusive forces is another revealed characteristic driver of streamflow hysteresis.

When put into perspective with the flow variables (recall, they peak in order of *WSS*, *V*, *Q*, then *WL* in hysteretic conditions), the dynamic term peaks near the peaks of *V* and *Q*, before the bulk terms, which are last, even after *WL* peaks (Figures 13-14). There is not a perfect match with the momentum term variable peak phasing because the hydraulic variables are involved in several terms of the dynamic equation (2). The earlier peaking of dynamic-based variables in hysteretic streamflow has implications for improved monitoring and forecasting of flood waves in most natural riverine systems.

5 Conclusion

With detailed physics-based model-simulated data, this study aims to add to the scientific understanding of streamflow hysteresis development and recommends improved streamflow monitoring and forecasting strategies. In a complementary effort to an exploration of typical flow variables, an analysis of the underlying momentum terms and their ingredients during a storm event provides a deeper understanding of streamflow hysteresis.

A detailed exploration of the St Venant terms during a fluvial flood wave cycle reveals the important drivers of streamflow hysteresis. While kinetic terms are dominant and balanced in non-hysteretic streamflow, hysteretic streamflow has an active pressure gradient and convective acceleration forces. We infer that hysteretic behavior may be possible if the wave is non-kinematic, meaning active pressure gradient and inertia terms may be included to solve the momentum equation, and flow is classified as diffusive or dynamic. The hysteresis behavior forms if the pressure gradient term is comparable in magnitude to the kinematic terms, and the convective acceleration term is active and within one or two orders of magnitude of the kinematic and diffusive terms.

In non-hysteretic streamflow conditions, kinematic flow is occurring, so it is acceptable to estimate flow using simple unique stage-discharge relationships. However, in hysteretic streamflow conditions, the active pressure gradient and convective acceleration terms must be accounted for to accurately capture the hysteresis loop in streamflow monitoring. It is increasingly feasible to measure these diffusive and dynamic variables with evolving monitoring technology. With improved monitoring protocols and instrumentation deployments that do not require operators in the field, it is even possible to measure those terms in the St Venant equation that are important to hysteretic streamflow, such as the water surface slope and convective acceleration. This analysis is valuable in informing the strategy to be adopted for accurate measurements in unsteady flows and rethinking the practical configurations for the monitoring methods that can capture the hysteretic features within reasonable cost-benefit margins.

Improvements in streamflow monitoring provide the opportunity for high-accuracy sediment monitoring, as estimates of sediment load through rivers depend directly on streamflow data. In fact, streamflow estimates are the building blocks for a wide range of applications (water quality constituents, reservoir management, etc.). Errors in flow estimates on the order of over 50% can have even greater implications when propagated to sediment and water quality studies. Quantifying the lag time between flow variables and repeating the experiment for a robust selection of locations and flood events results in the parameterization of streamflow hysteresis by a budget of the momentum terms. Further simulations of different events and locations along the Illinois River than those highlighted here confirm the findings.

There is also great utility in the revealed characteristics of hysteresis for advancements in streamflow forecasting capabilities, as the momentum term budget has direct implications to channel flow routing. Notably, the in-depth parameterization of streamflow hysteresis may open the door to more physics-based strategies for real-time data assimilation in forecasting modeling which captures the relevant flow dynamics. For example, the dynamic terms, water surface slope, and velocity peaking early in hysteretic conditions can be great predictors for machine learning streamflow forecasting algorithms. In improving our understanding of streamflow hysteresis, new opportunities are available for more comprehensive and physics-informed streamflow monitoring and forecasting protocol.

Acknowledgments

- This paper is based upon work supported by the National Science Foundation under Grant No. 2139663.
- Special thanks to Nazmul Beg for his dedicated guidance and foundational work put in during the initiation of this study.

Open Research

Availability Statement for underlying data and code:

- The data used for input to RAS models for all boundary conditions are from publicly sourced databases:
    - The United States Geological Survey (USGS) Water Data for the Nation via http://dx.doi.org/10.5066/F7P55KJN, http://waterdata.usgs.gov/nwis/ with public access conditions.
    - The United States Army Corps of Engineers (USACE) RiverGages.com via https://rivergages.mvr.usace.army.mil/WaterControl/new/layout.cfm with public access conditions.
    - The National Weather Service (NWS) North Central River Forecast Center (NCRFC) via https://www.weather.gov/ncrfc/ with access conditions by request.

Availability Statement for the software and other research products:

- The HEC-RAS model (software v6.1) used as the foundation of this study representing the complex IL River is preserved at USACE UMR Hydraulic Model Update webpage https://www.mvr.usace.army.mil/Missions/Flood-Risk-Management/UMRS-Hydraulic-Model-Update/, available upon request to Federal, state, local agencies, and NGOs along with their engineering consultants (USACE, 2022).
- Version 6.2 of the publicly available HEC-RAS software used for developing the reduced complexity models is preserved at https://www.hec.usace.army.mil/software/hec-ras/download.aspx, available via public access conditions.

References

Cheng, Z., Lee, K., Kim, D., Muste, M., Vidmar, P., & Hulme, J. (2019). Experimental evidence on the performance of rating curves for continuous discharge estimation in complex flow situations. *Journal of Hydrology*, 568, 959-971. doi:10.1016/j.jhydrol.2018.11.021

De St Venant, B. (1871). Theorie du mouvement non-permanent des eaux avec application aux crues des rivers et a l'introduntion des Marees dans leur lit. Academic de Sci. Comptes Redus, 73(99), 148-154.

Demir, I., Xiang, Z., Demiray, B., & Sit, M. (2022). WaterBench-Iowa: a large-scale benchmark dataset for data-driven streamflow forecasting. Earth system science data, 14(12), 5605-5616.

Dottori, F., Martina, M. L. V., and Todini, E.: A dynamic rating curve approach to indirect discharge measurement, *Hydrol. Earth Syst. Sci.*, 13, 847–863. doi:10.5194/hess-13-847-2009, 2009.

Fenton, J. D. (2001). Rating curves: Part 1 - Correction for surface slope, in Proc. Conf. on Hydraulics in Civil Engng, 28-30 Nov., Inst. Engnrs, Aust., Hobart, pp. 309-317.

Ferrick, M. G. (1985). Analysis of river wave types. *Water Resources Research*, 21(2), 209-220. doi:10.1029/WR021i002p00209

Follansbee, R., 1994. A history of the Water Resources Branch, U.S. Geological Survey; Volume I, from predecessor surveys to June 30, 1919.

Fread, D. L. (1975). Computation of Stage-Discharge Relationships Affected by Unsteady Flow. *Journal of the American Water Resources Association*, 11(2), 213-228. doi:10.1111/j.1752-1688.1975.tb00674.x

Graf, W. H., & Qu, Z. (2004, March). Flood hydrographs in open channels. In Proceedings of the institution of civil engineers-*Water management* (Vol. 157, No. 1, pp. 45-52). Thomas Telford Ltd. doi:10.1680/wama.2004.157.1.45

Green, J. (2005). Comparison of blockage factors in modelling the resistance of channels containing submerged macrophytes. *Rivers Research and Applications*, 21, 671–686. doi:10.1002/rra.854

Henderson, F.M. (1966). Open Channel Flow. Macmillan Series in Civil Engineering; Macmillan Company: New York, NY, USA, p. 522.

Holmes R (2016) River rating complexity. River Flow 2016, :679–686. doi:10.1201/9781315644479-107

Jones, C.S., Davis, C.A., Drake, C.W., Schilling, K.E., Debionne, S.H., Gilles, D.W., Demir, I. and Weber, L.J., (2018). Iowa statewide stream nitrate load calculated using in situ sensor network. JAWRA Journal of the American Water Resources Association, 54(2), pp.471-486.

Kennedy, E. (1984). Discharge ratings at gaging stations: US Geological Survey Techniques of Water-Resources Investigations, book 3, chap. A10, 59.

Knight, D.W. (2005). River flood hydraulics: validation issues in one-dimensional flood routing models.

Krajewski, W. F., Ghimire, G. R., Demir, I., & Mantilla, R. (2021). Real-time streamflow forecasting: AI vs. Hydrologic insights. Journal of Hydrology X, 13, 100110.

Lee, K., Firoozfar, A. R., and Muste, M (2017) Technical Note: Monitoring of unsteady open channel flows using the continuous slope-area method, *Hydrol. Earth Syst. Sci.*, 21, 1863–1874. doi:10.5194/hess-21-1863-2017

Levesque, V. A., & Oberg, K. A. (2012). Computing discharge using the index velocity method (pp. 3-A23). US Department of the Interior, US Geological Survey.

Li, Z., & Demir, I. (2022). A comprehensive web-based system for flood inundation map generation and comparative analysis based on height above nearest drainage. Science of The Total Environment, 828, 154420.

Meselhe, E.A. and Holly, F.M. Jr. (1997) "Invalidity of the Preissmann Scheme for Transcritical Flow," Journal of Hydraulic Engineering, ASCE, vol. 123(7). doi:10.1061/(ASCE)0733-9429(1997)123:7(652)

Meselhe, E., Lamjiri, M. A., Flint, K., Matus, S., White, E. D., & Mandli, K. (2021). Continental scale heterogeneous channel flow routing strategy for operational forecasting models. *Journal of the American Water Resources Association*, 57(2), 209-221. doi:10.1111/1752-1688.12847

Muste, M., Bacotiu, C., & Thomas, D. (2019). Evaluation of the slope-area method for continuous streamflow monitoring. In Proceedings of the 38th IAHR World Congress (pp. 121-130). doi:10.3850/38WC092019-1860

Muste, M., & Kim, D. (2020). Augmenting the Operational Capabilities of SonTek/YSI Streamflow Measurement Probes. Sontek/YSI-IIHR Collaborative Research Report.

Muste, M. and Kim, D. (2021). Augmenting the Operational Capabilities of SonTek/YSI Streamflow Measurement Probes. Sontek/YSIIIHR Collaborative Research Report. 2020. Available online: https://info.xylem.com/rs/240-UTB- 46/images/augmentingcapabilities-sontek-probe.pdf.

Muste, M., Kim, D., & Kim, K. (2022a). Insights into flood wave propagation in natural streams as captured with Acoustic Profilers at an index-velocity gaging station. *Water*, 14(9), 1380. doi:10.3390/w14091380

Muste, M., Kim, D., & Kim, K. (2022b). A flood-crest forecast prototype for river floods using only in-stream measurements. *Communications Earth & Environment*, 3(1), 78. doi:10.1038/s43247-022-00402-z

Muste, M., Kim, K., Kim, D. and Fleit G. (2024). Decoding the hysteretic behavior of hydraulic variables in lowland rivers with multivariate monitoring approaches, Submitted to Hydrological Processes, Special Issue on “Hydrological processes in lowlands and plains”.

Muste, M., Lee, K., Kim, D., Bacotiu, C., Rojas Oliveros, M., Cheng, Z. & Quintero, F. (2020) Revisiting hysteresis of flow variables in monitoring unsteady streamflows. *Journal of Hydraulic Research*, 58:6, 867-887. doi:10.1080/00221686.2020.1786742

Rantz, S. E. (1982). Measurement and computation of streamflow (Vol. 2175). US Department of the Interior, Geological Survey

Schmidt, A.R. (2002). Analysis of stage-discharge relations for open channel flows and their associated uncertainties. Ph.D. Thesis, University of Illinois at Urbana-Champaign, Champaign, IL, USA, 2002.

Schmidt, A. R. and Garcia, M. H. (2003). Theoretical Examination of Historical Shifts and Adjustments to Stage-Discharge Rating Curves. In P. Bizier, & P. DeBarry (Eds.), World Water and Environmental Resources Congress (pp. 1089-1098). (World Water and Environmental Resources Congress), DOI:10.1061/40685(2003)233

Sit, M., Demiray, B., & Demir, I. (2021). Short-term hourly streamflow prediction with graph convolutional gru networks. arXiv preprint arXiv:2107.07039.

Smith, C. F., Cordova, J. T. and Wiele, S. M. (2010). The continuous slope-area method for computing event hydrographs, U. S. Geological Survey Scientific Investigations Report 2010-5241, 37 p.

USACE, 2022. Upper Mississippi River Phase III Flood Risk Management Existing Conditions Hydraulic Model Documentation Report. https://www.mvr.usace.army.mil/Portals/48/docs/FRM/UMR%20Hydraulic%20Model%20Phase%20III%20-%20Report.pdf

Xu, H., Muste, M., & Demir, I. (2019). Web-based geospatial platform for the analysis and forecasting of sedimentation at culverts. Journal of Hydroinformatics, 21(6), 1064-1081.